Journal of the Optical Society of America A
OPTICS, IMAGE SCIENCE, AND VISION

Scintillation of partially coherent light in time-varying complex media

JOSSELIN GARNIER[1,3] AND KNUT SØLNA[2,4]

[1]Centre de Mathématiques Appliquées, Ecole Polytechnique, Institut Polytechnique de Paris, 91128 Palaiseau Cedex, France
[2]Department of Mathematics, University of California, Irvine, California 92697, USA
[3]e-mail: josselin.garnier@polytechnique.edu
[4]e-mail: ksolna@math.uci.edu

Received 10 January 2022; revised 13 May 2022; accepted 14 June 2022; posted 15 June 2022; published 5 July 2022

We present a theory for wave scintillation in the situation of a time-dependent partially coherent source and a time-dependent randomly heterogeneous medium. Our objective is to understand how the scintillation index of the measured intensity depends on the source and medium parameters. We deduce from an asymptotic analysis of the random wave equation a general form of the scintillation index, and we evaluate this in various scaling regimes. The scintillation index is a fundamental quantity that is used to analyze and optimize imaging and communication schemes. Our results are useful to quantify the scintillation index under realistic propagation scenarios and to address such optimization challenges. © 2022 Optica Publishing Group

https://doi.org/10.1364/JOSAA.453358

1. INTRODUCTION

We consider the fundamental problem of characterizing the scintillation of optical measurements with a time-dependent partially coherent source and a time-dependent random medium. The scintillation index corresponds to a measure of the signal-to-noise ratio or relative strength of fluctuations in intensity. If I is the measured intensity (irradiance), then we define the scintillation index by

$$\mathcal{S}=\frac{\mathbb{E}[I^2]-\mathbb{E}[I]^2}{\mathbb{E}[I]^2}, \tag{1}$$

where $\mathbb{E}[\cdot]$ stands for the statistical expectation obtained by averaging over repeated measurements under independent and identically distributed conditions. Modeling and analysis of laser speckle and scintillation are classic challenges in optics [1–3]. A rigorous mathematical analysis and quantification of scintillation has been a long standing open question despite the long history and importance of this challenge. General insight about what governs scintillation is important in the design of optical systems, for instance, for imaging and communication through a turbulent atmosphere [4] and through oceanic turbulence [5].

Here our focus is on a qualitative understanding about how the source and detector characteristic time scales affect scintillation. The related challenge of choosing appropriate specific source beams for scintillation control has also received a lot of attention [6,7]. The motivation for our paper is to consider simple models for the space and time covariance functions of the medium fluctuations and the source, which makes it possible to identify the different time and length scales of the problem and to carry out calculations to determine the dependence of the scintillation on these time and length scales. This approach is standard and gives insight about complex scattering situations in turbulent media [8]. Here we carry out a rigorous analysis of the equation that governs the fourth moments of the wave field and the scintillation index without approximation (such as a Gaussian approximation that makes it possible to express fourth-order moments in terms of second-order moments). In [9,10], we presented an analysis of the scintillation problem for deterministic coherent beams and plane wave sources and time-independent media. In this paper, we consider the scintillation problem when the source is partially coherent in time and space and the medium has time and space random fluctuations. Partially coherent sources have indeed been promoted for reducing scintillation at a receiving end in the context of laser propagation [6,11–13]. Most of these studies rely on physical experiments or numerics and Monte Carlo simulations to evaluate the scintillation index. From the theoretical point of view, analysis of wave propagation can be carried out in a perturbative regime using in particular Rytov theory with small fluctuations in the wave field to obtain insight about the scintillation [14,15]. The fluctuations of intensity and how they depend on source coherence time have been studied in [16,17] in the situation when the detector response time is either short or long compared to the source coherence time, but in general, short compared to the time scale at which the medium changes. We shall refer to the case when the detector averaging time is short, respectively, long, compared to the source coherence time as a fast, respectively, slow, detector. In [16,17], the case with a spatially coherent (plane wave) source is considered.

When turbulence is weak, the author uses an approximation in terms of a phase with Gaussian distribution to characterize the scintillation. When turbulence is strong he assumes a Gaussian field statistics to compute the fourth-order moment. In [18], this analysis is extended to the case when the source is also spatially incoherent (delta correlated) in a regime of weak turbulence. Similar analyses are carried out in [19,20], which address cases with slow and fast detectors and with a spatially incoherent source. In [21], it is shown how scintillation with a spatially partially coherent source can be enhanced by weak turbulence using the Rytov approximation. The case with a slow detector, but general spatial coherence, is considered in [22], which also considers application to communication and an explicit analysis of a bit error rate. Here we present an analysis that is valid also in the case of strong turbulence without using a Gaussian assumption for the distribution of wave field fluctuations and for general magnitudes of the detector response time and the source coherence radius and time as well as for the medium coherence time. A case with aperture averaging and small scintillation index is analyzed mathematically in [23] with a focus on how scintillation depends on the smoothness of the deterministic initial condition. Issues related to averaging are also considered in [24] in the context of deterministic sources by using a path integral approach for modeling the effect of turbulence.

In our paper, we consider the high-frequency situation where the effect of the random medium can be captured by a white-noise term in the Itô–Schrödinger equation that governs the evolution of the wave field [25,26]. This equation can address both weak intensity fluctuations and strong intensity fluctuations (saturated regime). The response time of the photodetector, the coherence times of the source, and the random medium can be arbitrary, provided that they are larger than the travel time of the field from the source to the detector through the medium. Under such circumstances, the effective reduced system (A13) for the fourth-order moments of the wave field can be derived from the Itô–Schrödinger equation and used for numerical evaluation of the scintillation index in the general high-frequency situation. Based on this system we here obtain explicit expressions of the scintillation index in three scaling regimes determined by the ratio of the correlation radius of the source over the correlation radius of the medium. We characterize scintillation with partially coherent sources and time-dependent random media and quantify how the space–time statistical parameters of the source and medium affect the scintillation index. An important aspect of our analysis is indeed that we allow the medium to be time dependent, so that it changes on a time scale that is slow relative to the travel time of the optical field. This is the situation in the context of laser beam propagation in the atmosphere with turbulence creating slow temporal changes of the medium. The detector in our modeling has a finite response time that can be on the time scale of the changes in the medium. The averaging at the detector can have a strong impact on the scintillation index depending on the characteristic time scales involved.

The configuration that we consider is illustrated in Fig. 1 with a partially coherent source field impinging from the left and propagating through a random medium, and then the scintillating intensity pattern is recorded at the receiver end.

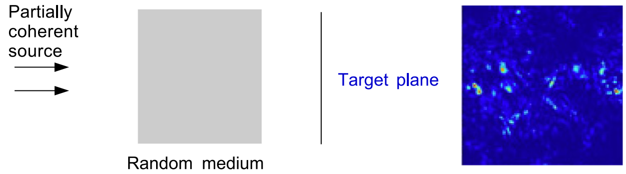

Fig. 1. Configuration that we consider. A partially coherent source fluctuating randomly in space and time is impinging on a complex medium from the left, and the intensity pattern is recorded at the receiver end to the right.

The complex medium is modeled as random and changes in space and time. The time changes in the medium happen on the recording time scale of the detector, but are slow relative to the travel time of the wave over the considered range. Due to time averaging, the detector measures a smoothed version of the intensity, and we seek to characterize the scintillation index of this measurement, which corresponds to a signal-to-noise ratio. We assume here scalar wave propagation and model the random medium in terms of the random fluctuations in the index of refraction; moreover, we assume no absorption. The scattering associated with the index of refraction fluctuations produces a scrambling of the wave field as it propagates. Thus, we have two sources of randomness in that the source field is partially coherent and modeled as a random field itself, which is then further randomized due to the medium fluctuations. Our objective is to characterize the scintillation index of the observed transmitted intensity pattern shown to the right in the figure.

We comment on a special, but important, case corresponding to the wave field having a Gaussian distribution. Indeed it is a well-accepted conjecture that the statistics of the complex wave field becomes circularly symmetric complex Gaussian when the wave propagates through a turbulent atmosphere [27,28], and the conjecture can be proved in certain situations [29–31]. In the Gaussian case, the intensity is the sum of the squares of two independent Gaussian random variables, which up to a scaling has χ-square distribution with two degrees of freedom, that is, an exponential distribution. This situation gives a unit scintillation index. Based on an analysis of the fourth moment of the wave field, we identify in this paper regimes that correspond to a unit value for the scintillation index and that are consistent with the Gaussian conjecture. The case with a field with Gaussian statistics is the critical situation with the signal-to-noise ratio of the intensity being one. In general, the scintillation index can be below one for small fluctuations in intensity and can reach values beyond one when the intensity distribution has heavier tails than those corresponding to the exponential distribution. We encounter both situations in this paper and discuss what type of scaling regime may lead to such situations. It is one of the main points of the paper to show that the analysis of the second-order moments of the intensity (or fourth-order moments of the wave field) depends on parameters that are not the ones that determine the behavior of the second-order moments.

The outline of the paper is as follows. We formulate the problem in Section 2. This involves defining the statistical models for the source and the medium and deriving the stochastic partial differential equation, the Itô–Schrödinger equation, that characterizes the wave field. We then relate the solution of the stochastic partial differential equation to the measured scintillation index. The main theoretical foundation for analyzing the scintillation is a framework for analyzing the fourth-order moment of the wave field, and we discuss this in Section 3. In Section 4, we give the main results that characterize the scintillation index in various scaling regimes. In Section 5, we present an example involving data presented in [12]. Technical calculations associated with the fourth-order moment equations are presented in the appendices.

2. PROBING TIME-DEPENDENT COMPLEX MEDIA WITH PARTIALLY COHERENT SOURCES

In this section, we outline the modeling and the problem that we will consider. In Section 2.A, we describe the statistical modeling of the source and of the random medium. In Section 2.B, we give the Itô–Schrödinger equation that describes the evolution of the wave field in the random medium. In Section 2.C, we relate the random transmitted wave field to the quantity of interest, which is the scintillation index of the measurements.

A. Source and Medium Modeling

The time-harmonic field $U(z, \boldsymbol{x}, t)$ satisfies the Helmholtz equation

$$\Delta U + k_o^2 n^2(z, \boldsymbol{x}, t) U = -\delta(z) f(\boldsymbol{x}, t), \quad (z, \boldsymbol{x}) \in \mathbb{R} \times \mathbb{R}^2, \tag{2}$$

where $k_o = 2\pi/\lambda_o$ is the central wavenumber (λ_o is the central wavelength). Here t is the slow time corresponding to the time at which the random medium and the source change. Furthermore, $\Delta = \partial_{x_1}^2 + \partial_{x_2}^2 + \delta_z^2$ is the Laplacian in the spatial variables. The coherence times of the medium and source are assumed to be much larger than the travel time from the source to the detector through the medium, so that t is a frozen parameter in Eq. (2).

The source f in the plane $z = 0$ is partially coherent, statistically stationary in space and time. We model it as a complex Gaussian process with mean zero, variance one, and covariance:

$$\mathbb{E}\left[f\left(\boldsymbol{x} + \frac{\boldsymbol{y}}{2}, t + \frac{\tau}{2}\right) \bar{f}\left(\boldsymbol{x} - \frac{\boldsymbol{y}}{2}, t - \frac{\tau}{2}\right)\right]$$
$$= F\left(\frac{\tau}{\tau_s}\right) \exp\left(-\frac{|\boldsymbol{y}|^2}{4\ell_s^2}\right), \tag{3}$$

where the bar represents complex conjugation, ℓ_s, respectively, τ_s, is the correlation radius, respectively, the coherence time, of the source, and the time covariance function F is normalized so that $F(0) = 1$ and $\int_0^\infty F(s)\mathrm{d}s = \mathcal{O}(1)$. We may use $F(s) = \exp(-s^2/4)$, for instance. Here the correlation radius of the source ℓ_s is assumed to be small relative to the range L, and the coherence time τ_s is assumed to be much larger than the propagation time L/c_o, where c_o is the background speed of propagation, and L is the distance from the source to the detector. For convenience, we use here a Gaussian correlation function for the spatial source correlations, but we remark that we could have used a more general form. A more detailed model for the source, in particular a discussion of realization via spatial light modulators (SLMs) can be found in [11,32]. For other approaches to the generation of the partially coherent source, we refer to [33], for instance.

The medium is random, and we denote by ν the relative fluctuations in the square index of refraction: $n^2(z, \boldsymbol{x}, t) = 1 + \nu(z, \boldsymbol{x}, t)$. The stochastic process ν is stationary in space and time and zero-mean, and its covariance function is of the form

$$\mathbb{E}[\nu(z' + z, \boldsymbol{x}' + \boldsymbol{x}, t + \tau)\nu(z', \boldsymbol{x}', t)]$$
$$= \sigma_m^2 G\left(\frac{\tau}{\tau_m}\right) \mathcal{C}_m\left(\frac{z}{\ell_m}, \frac{\boldsymbol{x}}{\ell_m}\right), \tag{4}$$

where ℓ_m, resp. τ_m, is the correlation radius, resp., the coherence time, of the random medium fluctuations, σ_m is the standard deviation of the fluctuations of the square index of refraction, and functions G and $\mathcal{C}_m$ are normalized so that $G(0) = 1$, $\int_0^\infty G(s)\mathrm{d}s = 1$, $\mathcal{C}_m(0, \boldsymbol{0}) = 1$, $\int_{\mathbb{R}} \mathcal{C}_m(\zeta, \boldsymbol{0})\mathrm{d}\zeta = 1$, and $\int_{\mathbb{R}^2} \mathcal{C}_m(0, \boldsymbol{\chi})\mathrm{d}\boldsymbol{\chi} = 1$. The special case where the correlation function corresponds to Kolmogorov turbulence is discussed in [34]. Here the correlation radius of the random medium ℓ_m is assumed to be small relative to the range L, and the coherence time of the medium τ_m is assumed to be much larger than the propagation time L/c_o. Thus, the "turnover time" of the medium is long compared to the propagation time; however, we assume that it may be on the scale of the coherence time of the source τ_s. Our interest is now in determining how the characteristics of these source and medium statistics determine the scintillation index of the transmitted wave field. We discuss next the equation that can be used to describe the evolution of the statistics of the wave field, that is, the equation that describes how the interaction with the random medium modifies the statistical distribution of the wave field.

B. Itô–Schrödinger Equation

The complex amplitude field u that modulates the carrier plane wave,

$$U(z, \boldsymbol{x}, t) = \frac{i}{2k_o} \exp(ik_o z) u(z, \boldsymbol{x}, t),$$

satisfies the Itô–Schrödinger equation [35]

$$\mathrm{d}u(z, \boldsymbol{x}, t) = \frac{i}{2k_o}\Delta_{\boldsymbol{x}} u(z, \boldsymbol{x}, t)\mathrm{d}z + \frac{ik_o}{2} u(z, \boldsymbol{x}, t) \circ \mathrm{d}B(z, \boldsymbol{x}, t), \tag{5}$$

with the initial condition in the plane $z = 0$:

$$u(z = 0, \boldsymbol{x}, t) = f(\boldsymbol{x}, t).$$

Here $\Delta_{\boldsymbol{x}}$ is the transverse Laplacian in $\boldsymbol{x}$, and t is the slow time scale corresponding to the time at which the source and the random medium change. The time t is a frozen parameter in Eq. (5). This is a consequence of our assumption that the coherence times of the source and of the medium are long relative to the travel time of the field over the range L. Equation (5) can also be written in the more familiar form ([36], Section 20.1)

$$\partial_z u(z, \boldsymbol{x}, t) = \frac{i}{2k_o}\Delta_{\boldsymbol{x}} u(z, \boldsymbol{x}, t) + \frac{ik_o}{2} u(z, \boldsymbol{x}, t)\dot{B}(z, \boldsymbol{x}, t), \tag{6}$$

provided we interpret $\dot{B}$ as a Gaussian process delta-correlated in z and compute moments involving products of the form $u\dot{B}$ by the Furutsu–Novikov formula ([36], Appendix 20.B). Equation (6) is also referred to as the Markov approximation in the physical literature [37,38]. The derivation of Eq. (5) from Eq. (2) is given in [9,35]. The derivation involves a limit theorem valid in the white-noise paraxial regime, when the wavelength is much smaller than the correlation radii of the source and of the medium, which are themselves much smaller than the propagation distance. Note that in Eq. (5) the symbol $\circ$ stands for the Stratonovich stochastic integral. There are, indeed, different definitions of the stochastic integral; the most standard definition is the Itô one, which is encountered in financial mathematics, for instance. In the Itô sense, Eq. (5) takes the form

$$\mathrm{d}u(z,\boldsymbol{x},t)=\frac{i}{2k_o}\Delta_{\boldsymbol{x}}u(z,\boldsymbol{x},t)\mathrm{d}z+\frac{ik_o}{2}u(z,\boldsymbol{x},t)\mathrm{d}B(z,\boldsymbol{x},t) - \frac{k_o^2\sigma_m^2\ell_m}{8}u(z,\boldsymbol{x},t)\mathrm{d}z. \tag{7}$$

The derivation of Eq. (5) from Eq. (2) clarifies that the stochastic integral that should be used for the Schrödinger Eq. (5) is Stratonovich, and this gives the familiar form Eq. (6). The derivation of Eq. (5) from Eq. (2) does not involve the assumption that the fluctuations of the index of refraction are Gaussian or delta-correlated. It follows from the derivation that the process $\dot{B}$ is Gaussian and delta-correlated. From Eq. (5) and Itô's formula, it becomes straightforward to derive closed equations for all moments as we will see below.

In Eq. (5), the process $B(z,\boldsymbol{x},t)$ is a real-valued Brownian field over $[0,\infty)\times\mathbb{R}^2\times\mathbb{R}$ with a covariance that derives from the model for the medium fluctuations in Eq. (4):

$$\mathbb{E}[B(z,\boldsymbol{x},t)B(z',\boldsymbol{x}',t')] = \sigma_m^2\ell_m\min\{z,z'\}G\left(\frac{t-t'}{\tau_m}\right)C\left(\frac{\boldsymbol{x}-\boldsymbol{x}'}{\ell_m}\right), \tag{8}$$

where $C(\boldsymbol{\chi})=\int_{\mathbb{R}}\mathcal{C}_m(\zeta,\boldsymbol{\chi})\mathrm{d}\zeta$, which is such that $C(\boldsymbol{0})=1$. The first- and second-order moments of the wave field are well known (see [36], Chapter 20] and references therein). They can also be obtained from the Itô–Schrödinger model Eq. (5) by Itô's formula [35,39]. The first-order moment of the wave field is zero. The second-order moment of the wave field (mutual coherence function) defined by

$$\mu_2(z,\boldsymbol{x},\boldsymbol{y};\tau)=\mathbb{E}\left[u\left(z,\boldsymbol{x}+\frac{\boldsymbol{y}}{2},t+\tau\right)\overline{u\left(z,\boldsymbol{x}-\frac{\boldsymbol{y}}{2},t\right)}\right] \tag{9}$$

satisfies [9]

$$\frac{\partial\mu_2}{\partial z}=\frac{i}{k_o}\nabla_{\boldsymbol{x}}\cdot\nabla_{\boldsymbol{y}}\mu_2+\frac{k_o^2\sigma_m^2\ell_m}{4}U_2(\boldsymbol{x},\boldsymbol{y};\tau)\mu_2, \tag{10}$$

with the potential $U_2(\boldsymbol{x},\boldsymbol{y};\tau)=G(\tau/\tau_m)C(\boldsymbol{y}/\ell_m)-1$ and the initial condition $\mu_2(z=0,\boldsymbol{x},\boldsymbol{y};\tau)=\mathbb{E}[f(\boldsymbol{x}+\boldsymbol{y}/2,t+\tau)\overline{f(\boldsymbol{x}-\boldsymbol{y}/2,t)}]$, which are both independent of $\boldsymbol{x}$. The second-order moment is given by

$$\mu_2(z,\boldsymbol{x},\boldsymbol{y};\tau)=F\left(\frac{\tau}{\tau_s}\right) \times\exp\left[-\frac{|\boldsymbol{y}|^2}{4\ell_s^2}-\frac{\sigma_m^2k_o^2\ell_m z}{4}\left(1-G\left(\frac{\tau}{\tau_m}\right)C\left(\frac{\boldsymbol{y}}{\ell_m}\right)\right)\right]. \tag{11}$$

By inspection of the behavior of the second-order moment when $\tau=0$,

$$\mathbb{E}\left[u\left(z,\boldsymbol{x}+\frac{\boldsymbol{y}}{2},t\right)\overline{u\left(z,\boldsymbol{x}-\frac{\boldsymbol{y}}{2},t\right)}\right] =\exp\left[-\frac{|\boldsymbol{y}|^2}{4\ell_s^2}-\frac{\sigma_m^2k_o^2\ell_m z}{4}\left(1-C\left(\frac{\boldsymbol{y}}{\ell_m}\right)\right)\right],$$

we find that the scattering mean free path ℓ_{sc} (that is, the typical propagation distance over which a coherent wave becomes incoherent) is

$$\ell_{\mathrm{sc}}^{-1}=\frac{\sigma_m^2k_o^2\ell_m}{4}. \tag{12}$$

Note that the scattering mean free path therefore is inversely proportional to the medium correlation length $\sigma_m^2\ell_m$. When C is smooth at zero, $C(\boldsymbol{\chi})=1-c_2|\boldsymbol{\chi}|^2+o(|\boldsymbol{\chi}|^2)$, the correlation radius $\rho_c(z)$ of the wave field is

$$\rho_c^{-2}(z)=\ell_s^{-2}+4c_2\frac{z}{\ell_{\mathrm{sc}}}\ell_m^{-2}. \tag{13}$$

By inspection of the behavior of the second-order moment when $\boldsymbol{y}=\boldsymbol{0}$,

$$\mathbb{E}[u(z,\boldsymbol{x},t+\tau)\overline{u(z,\boldsymbol{x},t)}] =F\left(\frac{\tau}{\tau_s}\right)\exp\left[-\frac{\sigma_m^2k_o^2\ell_m z}{4}\left(1-G\left(\frac{\tau}{\tau_m}\right)\right)\right],$$

we can see that when $F(s)=\exp(-s^2/4)$ and G is smooth at zero, $G(s)=1-g_2s^2+o(s^2)$, the coherence time $\tau_c(z)$ of the wave field is

$$\tau_c^{-2}(z)=\tau_s^{-2}+4g_2\frac{z}{\ell_{\mathrm{sc}}}\tau_m^{-2}. \tag{14}$$

Therefore, for deep probing, both the correlation radius and coherence time of the wave field are proportional to the reciprocal of the square root of the propagation distance. They both depend on the ratio of the propagation distance over the scattering mean free path. These calculations are valid as long as the white-noise, paraxial approximation is valid, that is to say, as long as $\rho_c(z)$ is larger than λ_o. By Eq. (13), this means that the propagation distance should be smaller than the transport mean free path:

$$\ell_{\mathrm{tr}}=\frac{\ell_m}{\sigma_m^2}. \tag{15}$$

We discuss next the measurements of intensity associated with the field u and the associated scintillation index.

C. Measurements and the Challenge of Understanding Scintillation

The intensity at lateral location $\boldsymbol{x}$ in the plane $z = L$ of the photodetector is

$$I_T(\boldsymbol{x}) = \frac{1}{T}\int_0^T |u(L, \boldsymbol{x}, t)|^2 \mathrm{d}t. \tag{16}$$

The intensity profile forms a smoothed speckle pattern. This smoothed speckle pattern depends in particular on the values of the integration time T, and coherence times of the source τ_s and of the medium τ_m, and we aim to understand how.

The empirical scintillation index measured by the photodetector of total aperture A is

$$\mathcal{S} = \frac{\frac{1}{|A|}\int_A I_T(\boldsymbol{x})^2 \mathrm{d}\boldsymbol{x} - \left(\frac{1}{|A|}\int_A I_T(\boldsymbol{x})\mathrm{d}\boldsymbol{x}\right)^2}{\left(\frac{1}{|A|}\int_A I_T(\boldsymbol{x})\mathrm{d}\boldsymbol{x}\right)^2}. \tag{17}$$

Here we have assumed that the detector has pixels that are smaller than the correlation radius of the beam. A more detailed model for the detector, in particular a discussion of the role of finite sized pixels of a (CCD) camera, can be found in, for instance, [12,40]. If the diameter of the photodetector aperture A is large (much larger than the correlation radius of the beam), then

$$\mathcal{S} = \frac{\mathbb{E}[I_T(\mathbf{0})^2] - \mathbb{E}[I_T(\mathbf{0})]^2}{\mathbb{E}[I_T(\mathbf{0})]^2}, \tag{18}$$

which is equal to

$$\mathcal{S} = \frac{2}{T}\int_0^T \left(1 - \frac{\tau}{T}\right) \frac{\mathrm{Cov}(|u(L, \mathbf{0}, 0)|^2, |u(L, \mathbf{0}, \tau)|^2)}{\mathbb{E}[|u(L, \mathbf{0}, 0)|^2]^2} \mathrm{d}\tau, \tag{19}$$

which is our quantity of interest. Note that the expectation here and below refers to expectation with respect to both the randomness of the medium and of the source. Note also that it follows from [9], Section 5, that $\mathbb{E}[|u(L, \mathbf{0}, t)|^2] = 1$. Therefore, to analyze $\mathcal{S}$, it remains to compute the fourth-order moment $\mathbb{E}[|u(L, \mathbf{0}, 0)|^2 |u(L, \mathbf{0}, \tau)|^2]$. We discuss the task of computing this moment next.

3. FOURTH-ORDER FIELD MOMENT AND SCINTILLATION

It is convenient to introduce the notation

$$f_\tau = F\left(\frac{\tau}{\tau_s}\right), \quad g_\tau = G\left(\frac{\tau}{\tau_m}\right). \tag{20}$$

We also introduce a notation for the fourth moment:

$$\begin{aligned}&\mu_4(z, \boldsymbol{x}_1, \boldsymbol{x}_2, \boldsymbol{y}_1, \boldsymbol{y}_2; \tau)\\ &= \mathbb{E}[u(z, \boldsymbol{x}_1, t+\tau)\overline{u(z, \boldsymbol{y}_1, t+\tau)}u(z, \boldsymbol{x}_2, t)\overline{u(z, \boldsymbol{y}_2, t)}].\end{aligned} \tag{21}$$

Here we focus on the fourth moment, while in [41], moments of all orders were considered under some simplifying assumptions of a different type. The fourth moment in Eq. (19) is a special case of the general fourth moment in Eq. (21) corresponding to evaluation at one spatial point only. The motivation for introducing the general fourth moment is that we can identify a partial differential equation satisfied by this general moment, and we will subsequently discuss the simplification that follows from evaluating this at particular values for the arguments. The general fourth moment satisfies the equation

$$\begin{aligned}\frac{\partial \mu_4}{\partial z} &= \frac{i}{2k_o}(\Delta_{\boldsymbol{x}_1} + \Delta_{\boldsymbol{x}_2} - \Delta_{\boldsymbol{y}_1} - \Delta_{\boldsymbol{y}_2})\mu_4\\ &+ \frac{k_o^2\sigma_m^2\ell_m}{4} U_4(\boldsymbol{x}_1, \boldsymbol{x}_2, \boldsymbol{y}_1, \boldsymbol{y}_2; \tau)\mu_4,\end{aligned} \tag{22}$$

with the generalized potential

$$\begin{aligned}U_4(\boldsymbol{x}_1, \boldsymbol{x}_2, \boldsymbol{y}_1, \boldsymbol{y}_2; \tau) &= C\left(\frac{\boldsymbol{x}_1 - \boldsymbol{y}_1}{\ell_m}\right) + C\left(\frac{\boldsymbol{x}_2 - \boldsymbol{y}_2}{\ell_m}\right)\\ &+ g_\tau C\left(\frac{\boldsymbol{x}_1 - \boldsymbol{y}_2}{\ell_m}\right) + g_\tau C\left(\frac{\boldsymbol{x}_2 - \boldsymbol{y}_1}{\ell_m}\right)\\ &- g_\tau C\left(\frac{\boldsymbol{x}_1 - \boldsymbol{x}_2}{\ell_m}\right) - g_\tau C\left(\frac{\boldsymbol{y}_1 - \boldsymbol{y}_2}{\ell_m}\right) - 2,\end{aligned} \tag{23}$$

and the initial condition

$$\begin{aligned}&\mu_4(z=0, \boldsymbol{x}_1, \boldsymbol{x}_2, \boldsymbol{y}_1, \boldsymbol{y}_2; \tau)\\ &= \mathbb{E}[f(\boldsymbol{x}_1, t+\tau)\overline{f(\boldsymbol{y}_1, t+\tau)}f(\boldsymbol{x}_2, t)\overline{f(\boldsymbol{y}_2, t)}].\end{aligned}$$

Equation (22) was derived and studied in [41–44] and [36], Section 20.13, for time-independent media, and the time-dependent case (with the frozen assumption) is a rather straightforward extension. Equation (22) follows from Eq. (5) using Itô calculus for Hilbert space valued processes [10,45]. Using the Gaussian property of the source and Isserlis formula (for the computation of high-order moments of the multivariate normal distribution in terms of its covariance matrix [46]), the initial condition for the fourth-order moment is

$$\begin{aligned}&\mu_4(z=0, \boldsymbol{x}_1, \boldsymbol{x}_2, \boldsymbol{y}_1, \boldsymbol{y}_2; \tau)\\ &= \exp\left(-\frac{|\boldsymbol{x}_1 - \boldsymbol{y}_1|^2}{4\ell_s^2} - \frac{|\boldsymbol{x}_2 - \boldsymbol{y}_2|^2}{4\ell_s^2}\right)\\ &+ f_\tau^2 \exp\left(-\frac{|\boldsymbol{x}_1 - \boldsymbol{y}_2|^2}{4\ell_s^2} - \frac{|\boldsymbol{x}_2 - \boldsymbol{y}_1|^2}{4\ell_s^2}\right).\end{aligned} \tag{24}$$

We can now express the quantity of interest, the scintillation index Eq. (19), in terms of the general fourth moment:

$$\mathcal{S} = \frac{2}{T}\int_0^T \left(1 - \frac{\tau}{T}\right) \frac{\mu_4(L, \mathbf{0}, \mathbf{0}, \mathbf{0}, \mathbf{0}; \tau) - \mu_2(L, \mathbf{0}, \mathbf{0}; 0)^2}{\mu_2(L, \mathbf{0}, \mathbf{0}; 0)^2} \mathrm{d}\tau, \tag{25}$$

where $\mu_2(L, \mathbf{0}, \mathbf{0}; 0) = \mathbb{E}[|u(L, \mathbf{0}, t)|^2] = 1$. Thus, it is the special fourth moment $\mu_4(L, \mathbf{0}, \mathbf{0}, \mathbf{0}, \mathbf{0}; \tau)$ that is needed to analyze the scintillation index. The explicit solution of the problem Eq. (22) is not known. In some scaling regimes, we can, however, identify asymptotic solutions using the framework introduced in [10]. In Appendix A, we discuss a fundamental transformation of the fourth-moment equation in Eq. (22) to a simplified problem from which the special fourth moment $\mu_4(L, \mathbf{0}, \mathbf{0}, \mathbf{0}, \mathbf{0}; \tau)$ derives.

4. SCINTILLATION IN CANONICAL SCALING REGIMES

We discuss here the three scaling regimes for scintillation. In these regimes, we can solve for the fourth moment in Eq. (22) explicitly. This allows us to get quantitative insight about the behavior of the scintillation and how it depends on the characteristic parameters in the problem, and we comment on this in detail. The first two regimes are particular cases of the far-field (or Fraunhofer) regime $\frac{\lambda_o L}{\min(\ell_s, \ell_m)^2} \gg 1$, when $L \gtrsim \ell_{\text{sc}}$. The third regime is a special Fresnel regime $\frac{\lambda_o L}{\min(\ell_s, \ell_m)^2} \sim 1$, when $L \gg \ell_{\text{sc}}$. The parameter determining the different regimes of scintillation is the ratio of the correlation radius ℓ_s of the source over the correlation radius ℓ_m of the medium fluctuations. If we address a multiscale medium such as a turbulent medium with a Kolmogorov spectrum, then we may think that the regime $\ell_s \sim \ell_m$ is the relevant one, as the wave will be affected mostly by the structures with the same scale as its correlation radius [47]. The analysis of the three canonical regimes $\ell_s \gg \ell_m$, $\ell_s \sim \ell_m$, $\ell_s \ll \ell_m$ goes beyond the Kolmogorov spectrum and makes it possible to clarify the roles of the different scales.

A. Source with Large Correlation Radius

We consider first the regime in which the correlation radius ℓ_s of the source is larger than the correlation radius of the medium ℓ_m, so that $\frac{\lambda_o L}{\ell_m^2} \gg 1$ but $\frac{\lambda_o L}{\ell_m \ell_s} \lesssim 1$. We carry out the analysis of this regime in Appendix B.1 where we derive the following expression for the scintillation index Eq. (25):

$$\mathcal{S} = \frac{2}{T} \int_0^T \left(1 - \frac{\tau}{T}\right) \times \left[f_\tau^2 \exp\left(-2\frac{(1-g_\tau)L}{\ell_{\text{sc}}}\right) + \mathcal{Q}_{g_\tau}(L) + f_\tau^2 \mathcal{Q}_1(L) \right] \mathrm{d}\tau, \tag{26}$$

where

$$\mathcal{Q}_g(L) = \exp\left(-2\frac{L}{\ell_{\text{sc}}}\right) \frac{1}{2\pi} \int_{\mathbb{R}^2} \exp\left(-\frac{|\boldsymbol{s}|^2}{2}\right) \times \left[\exp\left(2\frac{L}{\ell_{\text{sc}}} g \int_0^1 C\left(\frac{L\boldsymbol{s}s'}{k_o \ell_m \ell_s}\right) \mathrm{d}s'\right) - 1 \right] \mathrm{d}\boldsymbol{s}. \tag{27}$$

When $\frac{\lambda_o L}{\ell_m \ell_s} \ll 1$, the expression is simpler:

$$\mathcal{Q}_g(L) = \exp\left(-2\frac{L}{\ell_{\text{sc}}}(1-g)\right) - \exp\left(-2\frac{L}{\ell_{\text{sc}}}\right),$$

which depends only on the scattering mean free path. In general, for $\frac{\lambda_o L}{\ell_m \ell_s} \lesssim 1$, the function Eq. (27) depends on the two-point statistics of the random medium fluctuations and reflects their cumulative effects onto the wave propagation over the propagation distance L. Note that $g = 0$ corresponds to the situation with intensities of wave fields having propagated through uncorrelated random media and that indeed $\mathcal{Q}_0(L) = 0$.

The first term in the square brackets in Eq. (26) corresponds to the scintillation contribution from the fluctuations of the source, and this contribution is damped by temporal decorrelation of the medium fluctuations as well as temporal averaging at the detector. The second term in the square brackets is the scintillation contribution produced by the random medium fluctuations and is again damped by temporal decorrelation of the random medium fluctuations. The last term in the square brackets is a cross term reflecting the scintillation contribution from the combined effect of medium and source fluctuations.

We next discuss the behavior of the scintillation index in various special cases.

- Note first that a rapid decay of f_τ corresponds to rapid decorrelation of the source in time. Such a rapid decorrelation serves to reduce the scintillation index due to averaging by the photodetector. Similarly, a rapid decay of g_τ corresponds to rapid decorrelation in the medium fluctuations and reduced scintillation due to averaging over incoherent contributions. We find from Eq. (26) that when T becomes much larger than the coherence times of the source and of the medium, and assuming that $\tau \mapsto f_\tau \in L^2$ (i.e., is square-integrable) and that g_τ goes to zero at infinity fast enough so that $\tau \mapsto \mathcal{Q}_{g_\tau}(L) \in L^1$ (i.e., is integrable), then we have

$$\mathcal{S} \simeq 0$$

for any propagation distance.
- When the response time T of the detector is smaller than the coherence time of the medium, we have $g_\tau \equiv 1$ for all $\tau \in [0, T]$. In other words, the medium is frozen on the response time window of duration of the detector. We then have

$$\frac{\mu_4(L, \mathbf{0}, \mathbf{0}, \mathbf{0}, \mathbf{0}; \tau) - \mu_2(L, \mathbf{0}, \mathbf{0})^2}{\mu_2(L, \mathbf{0}, \mathbf{0})^2} = f_\tau^2 + (1 + f_\tau^2)\mathcal{Q}_1(L), \tag{28}$$

for all $\tau \in [0, T]$. This implies that when τ is larger than the source coherence time, the initial fields at two times separated by τ are independent ($f_\tau = 0$), but the intensities of the transmitted fields at two such times are correlated. Under such circumstances, the correlation degree Eq. (28) is zero at $L = 0$, it is not zero for positive L, and it goes to zero as $L \to +\infty$. When τ is smaller than or of the same order as the source coherence time, the initial fields at two times separated by τ are correlated and the transmitted intensities are correlated with the correlation degree Eq. (28). As a consequence, the scintillation index is given by

$$\mathcal{S} = \frac{2}{T} \int_0^T \left(1 - \frac{\tau}{T}\right) [f_\tau^2 + (1 + f_\tau^2)\mathcal{Q}_1(L)] \mathrm{d}\tau, \tag{29}$$

so that when T becomes much larger than the coherence time of the source, and assuming that $f_\tau \in L^2$, then we have

$$\mathcal{S} \simeq \mathcal{Q}_1(L).$$

This shows that the scintillation index corresponding to averaging of the initial incoherent intensity is zero, while the one corresponding to the transmitted intensity is not.

• When the response time T of the detector is smaller than both the coherence times of the source and the medium, we have $f_\tau = g_\tau = 1$ for all $\tau \in [0,\ T]$, and we have

$$\mathcal{S} = \frac{\mu_4(L, \mathbf{0}, \mathbf{0}, \mathbf{0}, \mathbf{0}; 0) - \mu_2(L, \mathbf{0}, \mathbf{0}; 0)^2}{\mu_2(L, \mathbf{0}, \mathbf{0}; 0)^2} = 1 + 2\mathcal{Q}_1(L). \quad (30)$$

Thus, initially the scintillation index is one (because the source has Gaussian distribution), then it reaches beyond one in a mixing region and returns to one for large propagation distances. Indeed, the fluctuations of the initial field happen on a spatial scale that is large relative to the scale of the field variations imposed by the random medium fluctuations resulting in a non-Gaussian mixture situation with a scintillation index beyond one.

• Consider the regime where the propagation distance is larger than the scattering mean free path:

$$\alpha_L := 2\frac{L}{\ell_{\mathrm{sc}}} \gg 1, \quad (31)$$

so that in the case of coherent sources, most of the wave energy has been transferred to incoherent wave energy. We will in this context assume that C is smooth and isotropic, so that we have (remember $C(\mathbf{0}) = 1$)

$$C(\boldsymbol{\chi}) = 1 - c_2|\boldsymbol{\chi}|^2 + o(|\boldsymbol{\chi}|^2). \quad (32)$$

Then we we can compute a simplified expression for $\mathcal{Q}_g(L)$ and find

$$\mathcal{Q}_g(L) \overset{\alpha_L \gg 1}{\simeq} \exp\left(-2\frac{L}{\ell_{\mathrm{sc}}}(1-g)\right) \frac{1}{1 + \frac{c_2\sigma_m^2 L^3 g}{3\ell_m \ell_s^2}}, \quad (33)$$

so that $\mathcal{Q}_1(L)$ goes to zero when the propagation distance L becomes larger than the critical length:

$$\ell_c := \sigma_m^{-2/3} \ell_m^{1/3} \ell_s^{2/3}, \quad (34)$$

which is not the scattering mean free path, nor the transport mean free path. It is larger than the scattering mean free path because $\ell_c^{3/2}/\ell_{\mathrm{sc}}^{3/2} \sim (\ell_m \ell_s)/(\ell_{\mathrm{sc}}\lambda_o) \gg (\ell_m \ell_s)/(L\lambda_o) \gtrsim 1$, and smaller than the transport mean free path because $\ell_c^{3/2}/\ell_{\mathrm{tr}}^{3/2} \sim \ell_s/\ell_{\mathrm{tr}} \ll 1$.

In Fig. 2, we illustrate the behavior of scintillation in the regime $\ell_s \gg \ell_m$, so that the lateral coherence scale of the source is larger than the correlation range of the medium. The figure shows how the scintillation index in Eq. (30) depends on the propagation distance. We introduce the length parameter

$$\ell = \frac{\ell_m \ell_s}{\lambda_o}.$$

Then we show the scintillation index as a function of L/ℓ for three different values of the parameter

$$\alpha_\ell = 2\frac{\ell}{\ell_{\mathrm{sc}}},$$

when $C(\boldsymbol{\chi}) = \exp(-|\boldsymbol{\chi}|^2/2)$. Note that with stronger medium fluctuations, the maximum value for the scintillation index is larger and happens for shorter propagation distances.

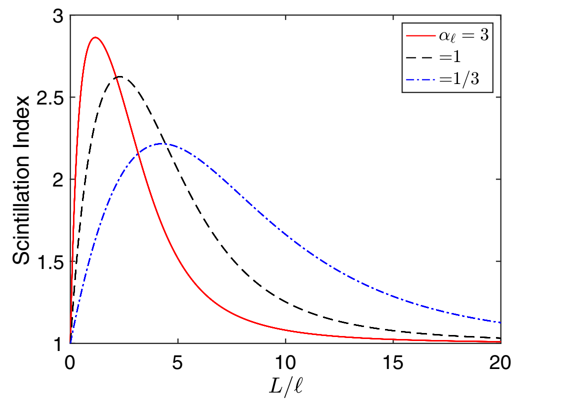

Fig. 2. Scintillation index $\mathcal{S}$ as a function of the relative propagation distance L/ℓ for three values of $\alpha_\ell = 2\ell/\ell_{\mathrm{sc}}$. The figure corresponds to the regime $\ell_s \gg \ell_m$ for small recording times at the detector (small means smaller than the coherence times of the source and of the medium) so that the scintillation index is given by Eq. (30).

B. Source with Intermediate Correlation Radius

We consider next the case when the correlation radius of the source is of the same order as the correlation radius of the medium, so that $\frac{\lambda_o L}{\ell_m^2} \gg 1$ and $\frac{\lambda_o L}{\ell_m \ell_s} \gg 1$. We carry out the analysis in Appendix B.2 where we derive the following expression for the scintillation index Eq. (25):

$$\mathcal{S} = \frac{2}{T}\int_0^T \left(1 - \frac{\tau}{T}\right)\left[f_\tau^2 \exp\left(-\frac{2(1-g_\tau)L}{\ell_{\mathrm{sc}}}\right)\right] \mathrm{d}\tau. \quad (35)$$

As above, the term in the square brackets corresponds to scintillation contribution from the fluctuations in the source, and this contribution is damped by fast temporal decorrelation of the medium fluctuations (small g_τ), moreover, by smoothing at the detector. Note that this term corresponds to the first term in the square brackets in Eq. (26). Indeed, the last two terms in the square brackets in Eq. (26) become small when ℓ_s is reduced, so that $\frac{\lambda_o L}{\ell_m \ell_s} \gg 1$. The situation with $\ell_s \sim \ell_m$ is the regime considered here. If we further reduce ℓ_s so that $\ell_s \ll \ell_m$, then we transition towards the regime considered in the next section. In the regime $\ell_s \sim \ell_m$, we can observe the following behaviors.

• In the case when T becomes much larger than the coherence time of the source, and assuming that $f_\tau \in L^2$, we have

$$\mathcal{S} \simeq 0$$

for any propagation distance due to averaging at the photodetector.

• For T smaller than the coherence times of both the source and the medium, we have $f_\tau = g_\tau = 1$ for all $\tau \in [0,\ T]$, and then

$$\mathcal{S} \simeq 1.$$

Here the field behaves as a complex Gaussian field, because the fluctuations in the source and in the medium happen at the same scale.

In Figs. 3 and 4, we illustrate the behavior of the scintillation index in the regime $\ell_s \sim \ell_m$. The figures show how the scintillation index depends on the magnitudes of the integration time at

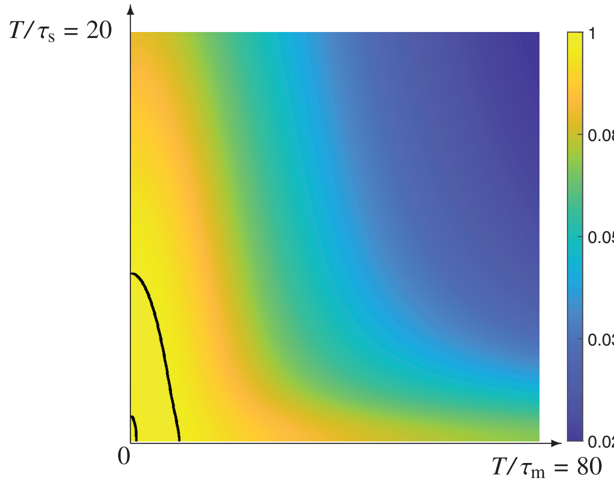

Fig. 3. Scintillation index $\mathcal{S}$ as a function of the coherence times of the source and of the random medium, plotted here as a function of T/τ_s and T/τ_m, with T the recording time of the detector, in the regime $\ell_s \sim \ell_m$[see Eq. (35)]. Here $\alpha_L = 2L/\ell_{sc} = 3$. The two solid black lines correspond to contour levels $\mathcal{S} = .8$ and .2. Note that here and below, we adapt the color scale to the particular distribution of scintillation index values.

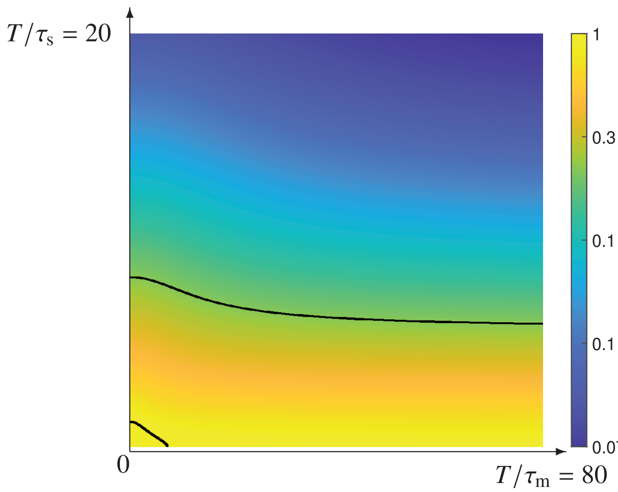

Fig. 4. As in Fig. 3, but here $\alpha_L = 2L/\ell_{sc} = 1/3$.

the detector relative to the coherence times of the source and of the medium. The two figures correspond to two different values for the parameter $\alpha_L = 2L/\ell_{sc}$. The time coherence functions f_τ and g_τ are chosen to be Gaussian:

$$f_\tau = \exp\left(-\frac{\tau^2}{2\tau_s^2}\right), \quad g_\tau = \exp\left(-\frac{\tau^2}{2\tau_m^2}\right). \tag{36}$$

Note how strong medium fluctuations serve to reduce the scintillation index in the case with a time-dependent random medium and temporal averaging at the detector, moreover, how also long duration detector temporal averaging serves to reduce the scintillation index.

C. Source with Small Correlation Radius

We finally consider the regime in which the correlation radius of the source is smaller than the correlation radius of the medium, and we have $\frac{\lambda_o L}{\ell_s^2} \lesssim 1$. A similar regime (called spot-dancing regime) has already been considered in the literature to study coherent and narrow beam propagation: the beam propagates with the same transverse profile as in a homogeneous medium, but its center randomly wanders, more exactly, its center is a random process whose standard deviation increases with propagation distance [9,48]. Here we also assume that C is smooth and isotropic with an expansion as in Eq. (32). We carry out the analysis in Appendix B.3 where we derive the following expression for the scintillation index Eq. (25):

$$\mathcal{S} = \frac{2}{T}\int_0^T \left(1 - \frac{\tau}{T}\right)\left[\frac{f_\tau^2}{1 + \frac{c_2 L^3}{\ell_c^3}(1 - g_\tau)}\right] d\tau, \tag{37}$$

where ℓ_c is defined by Eq. (34). The numerator within the square brackets corresponds to the scintillation contribution of the Gaussian source, while the denominator corresponds to damping of the scintillation index due to temporal decorrelation in the random medium. We can moreover make the following observations.

- When T becomes much larger than the coherence time of the source, and assuming that $f_\tau \in L^2$, then we have

$$\mathcal{S} \simeq 0$$

for any propagation distance. Note that the scintillation index is small even if the medium is frozen since the medium fluctuations do not strongly contribute to the intensity correlations with the very small source correlation radius.

- For T smaller than the coherence times of the source and of the medium, we have $f_\tau = g_\tau = 1$ for all $\tau \in [0, T]$, and it follows that

$$\mathcal{S} \simeq 1.$$

This corresponds to a Gaussian situation since the random medium fluctuations again do not strongly affect the correlations in this case with a source with rapid stationary spatial fluctuations. This is in contrast to the situation with a deterministic beam source when the spot-dancing property produces a heavy-tailed intensity distribution and large scintillation index (a non-central chi-square distribution with two degrees of freedom, also known as the Rice–Nakagami distribution [9]).

In Figs. 5 and 6, we illustrate the behavior of the scintillation index in the regime $\ell_s \ll \ell_m$. The figure shows how the scintillation index depends on the magnitudes of the coherence times of the source and of the medium relative to the integration time at the detector. The two figures correspond to two different values for the ratio of the propagation distance L over the critical length ℓ_c defined by Eq. (34), and we again assume a Gaussian time coherence function f_τ as in Eq. (36). As above, note how strong medium fluctuations serve to reduce the scintillation index in the case with a time-dependent random medium and temporal averaging at the detector, moreover, how again long detector temporal averaging serves to reduce the scintillation index.

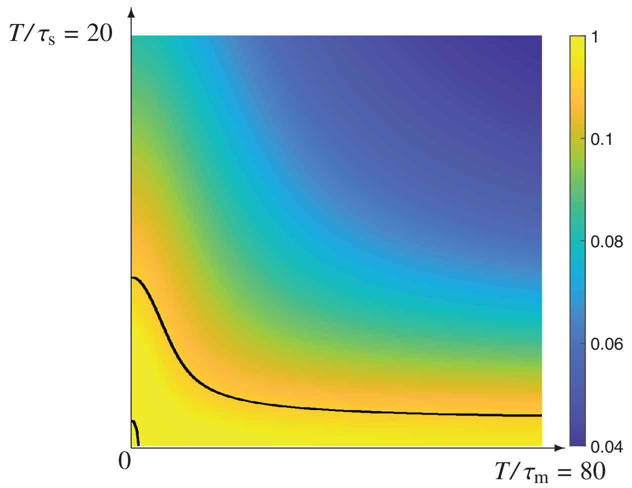

Fig. 5. Scintillation index $\mathcal{S}$ as a function of (reciprocal) coherence times of the source and of the random medium, respectively, τ_s and τ_m, relative to T, recording time of the detector, in the regime $\ell_s \ll \ell_m$ [see Eq. (37)]. Here $c_2 L^3/\ell_c^3 = 9$. The two solid black lines correspond to contour levels $\mathcal{S} = .8$ and .2.

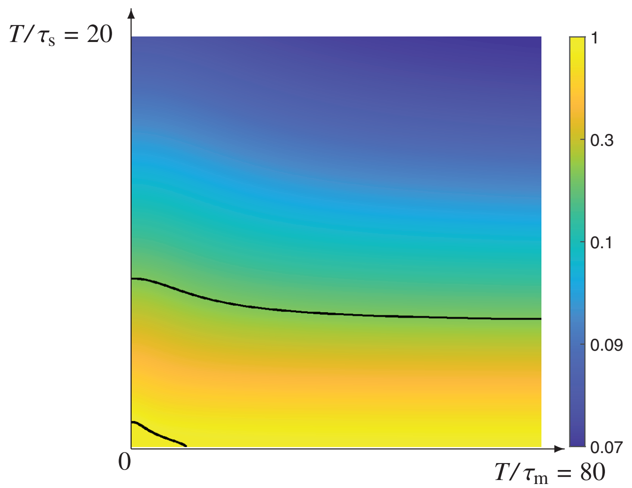

Fig. 6. As in Fig. 5, but with $c_2 L^3/\ell_c^3 = 1$.

5. EXAMPLE WITH EXPERIMENTAL DATA

We discuss an example with real data taken from [12] by Nelson *et al*. The experiment in [12] involves an over-the-water laser beam link at the United States Naval Academy. The source is partially coherent (multi-Gaussian Schell model) and realized via a SLM. The measurement procedure at the CCD camera corresponds to a recording time of $T = 60$ s. The experiment is carried out for various values for the source coherence time τ_s realized via varying the SLM cycling rate. The field trials were conducted in July and were performed during the night in calm weather conditions over a maritime link of 323 m. We refer to [12] for a more detailed description of the experimental setup. Assuming a frozen medium in view of calm weather, we can then model the observed scintillation index as in Eq. (29):

$$\mathcal{S} = \frac{2}{T}\int_0^T \left(1 - \frac{\tau}{T}\right) [f_\tau^2 + (1 + f_\tau^2)Q_1(L)]\mathrm{d}\tau \overset{\tau_s \ll T}{\to} \frac{d_1}{\tau_s^{-1}} + d_2, \tag{38}$$

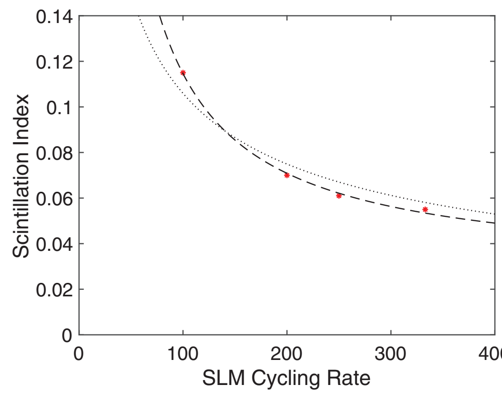

Fig. 7. Measurements of scintillation index as function of the SLM cycling rate (red stars). The observations conform well with the theoretical predictions in Eq. (29) (dashed line) assuming a frozen medium. The dotted line corresponds to fitting of the model in Eq. (39) taken from [18].

and we can fit the parameters d_1, d_2 via least squares. The results are shown in Fig. 7 by the dashed line, and we can see an excellent fit between model and data. The regime of a slow detector relative to the temporal source coherence time and with a short source spatial coherence scale and frozen medium was analyzed in [18] using the extended Huygens–Fresnel principle, and it gives the following scintillation model:

$$\mathcal{S} \simeq \frac{d_2}{\sqrt{1 + d_1 \tau_s^2}}. \tag{39}$$

By a least squares fit of d_1, d_2, we get the dotted line in Fig. 7.

6. CONCLUSION

We have considered the scintillation of a wave field that is observed after propagation through a time-dependent random medium. The source is partially coherent in time and space and constitutes a random field in lateral space and time variables. We consider a high-frequency and far-field regime. We give here precise characterizations of the scaling regimes leading to the different canonical forms of scintillation. The central scaling parameters are the temporal and spatial statistical coherence lengths of the source and of the random medium, in addition to the propagation range and the strength of random medium fluctuations, and the response time of the photodetector. In the high-frequency and far-field regime, three scaling regimes are identified depending on the magnitude of the spatial correlation radius of the source relative to that of the medium. We identify general formulas for the scintillation index in each regime and discuss special cases corresponding to an effective Gaussian situation with a scintillation index equal to one, a non-Gaussian mixture situation with a scintillation index reaching beyond one, and situations with a small scintillation index corresponding to a desirable high signal-to-noise ratio for the measured intensity. In particular, temporal averaging creates situations with a low scintillation index. In the context of, for instance, communication, however, long recording times are not in general desirable, and our analysis presents quantitative insights about appropriate trade-offs that can be made for optimal system performance. Such particular system optimization challenges are left for future work. We also remark that we have considered the case when the source has infinite lateral spatial extent and is a stationary stochastic process in lateral space coordinates and time. The case when the source is modulated by a finite source aperture and the associated challenge of identifying the spreading of the wave field and the evolution of speckle statistics can be analyzed via similar theoretical frameworks as those presented here, but is also left for future work.

APPENDIX A: ANALYSIS OF FOURTH-ORDER MOMENT EQUATIONS

The main equation underlying the above results is a simplified equation deriving from Eq. (22) and from which the expressions of the special fourth moments $\mu_4(L, \mathbf{0}, \mathbf{0}, \mathbf{0}, \mathbf{0}; \tau)$ follow. We deduce this equation here and analyze it in the specific scintillation regimes in Appendix B.

Consider the general moments in Eq. (21) satisfying Eq. (22) with initial condition Eq. (24). It will be convenient to parameterize the four points $\boldsymbol{x}_1, \boldsymbol{x}_2, \boldsymbol{y}_1, \boldsymbol{y}_2$ in Eq. (21) in a special way:

$$\boldsymbol{x}_1 = \frac{\boldsymbol{r}_1 + \boldsymbol{r}_2 + \boldsymbol{q}_1 + \boldsymbol{q}_2}{2}, \quad \boldsymbol{y}_1 = \frac{\boldsymbol{r}_1 + \boldsymbol{r}_2 - \boldsymbol{q}_1 - \boldsymbol{q}_2}{2}, \tag{A1}$$

$$\boldsymbol{x}_2 = \frac{\boldsymbol{r}_1 - \boldsymbol{r}_2 + \boldsymbol{q}_1 - \boldsymbol{q}_2}{2}, \quad \boldsymbol{y}_2 = \frac{\boldsymbol{r}_1 - \boldsymbol{r}_2 - \boldsymbol{q}_1 + \boldsymbol{q}_2}{2}. \tag{A2}$$

In particular, $\boldsymbol{r}_1/2$ is the barycenter of the four points $\boldsymbol{x}_1, \boldsymbol{x}_2, \boldsymbol{y}_1, \boldsymbol{y}_2$:

$$\boldsymbol{r}_1 = \frac{\boldsymbol{x}_1 + \boldsymbol{x}_2 + \boldsymbol{y}_1 + \boldsymbol{y}_2}{2}, \quad \boldsymbol{q}_1 = \frac{\boldsymbol{x}_1 + \boldsymbol{x}_2 - \boldsymbol{y}_1 - \boldsymbol{y}_2}{2},$$

$$\boldsymbol{r}_2 = \frac{\boldsymbol{x}_1 - \boldsymbol{x}_2 + \boldsymbol{y}_1 - \boldsymbol{y}_2}{2}, \quad \boldsymbol{q}_2 = \frac{\boldsymbol{x}_1 - \boldsymbol{x}_2 - \boldsymbol{y}_1 + \boldsymbol{y}_2}{2}.$$

We denote by μ the fourth-order moment in these new variables:

$$\mu(z, \boldsymbol{q}_1, \boldsymbol{q}_2, \boldsymbol{r}_1, \boldsymbol{r}_2; \tau) = \mu_4(z, \boldsymbol{x}_1, \boldsymbol{x}_2, \boldsymbol{y}_1, \boldsymbol{y}_2; \tau), \tag{A3}$$

with $\boldsymbol{x}_1, \boldsymbol{x}_2, \boldsymbol{y}_1, \boldsymbol{y}_2$ given by Eqs. (A1) and (A2) in terms of $\boldsymbol{q}_1, \boldsymbol{q}_2, \boldsymbol{r}_1, \boldsymbol{r}_2$.

In the variables $(\boldsymbol{q}_1, \boldsymbol{q}_2, \boldsymbol{r}_1, \boldsymbol{r}_2)$, the function μ satisfies the system

$$\frac{\partial \mu}{\partial z} = \frac{i}{k_o}(\nabla_{\boldsymbol{r}_1} \cdot \nabla_{\boldsymbol{q}_1} + \nabla_{\boldsymbol{r}_2} \cdot \nabla_{\boldsymbol{q}_2})\mu + \frac{\sigma_m^2 k_o^2 \ell_m}{4} U(\boldsymbol{q}_1, \boldsymbol{q}_2, \boldsymbol{r}_1, \boldsymbol{r}_2; \tau)\mu, \tag{A4}$$

with the generalized potential

$$U(\boldsymbol{q}_1, \boldsymbol{q}_2, \boldsymbol{r}_1, \boldsymbol{r}_2; \tau) = C\left(\frac{\boldsymbol{q}_2 + \boldsymbol{q}_1}{\ell_m}\right) + C\left(\frac{\boldsymbol{q}_2 - \boldsymbol{q}_1}{\ell_m}\right) + g_\tau C\left(\frac{\boldsymbol{r}_2 + \boldsymbol{q}_1}{\ell_m}\right) + g_\tau C\left(\frac{\boldsymbol{r}_2 - \boldsymbol{q}_1}{\ell_m}\right) - g_\tau C\left(\frac{\boldsymbol{q}_2 + \boldsymbol{r}_2}{\ell_m}\right) - g_\tau C\left(\frac{\boldsymbol{q}_2 - \boldsymbol{r}_2}{\ell_m}\right) - 2. \tag{A5}$$

The Fourier transform (in $\boldsymbol{q}_1, \boldsymbol{q}_2, \boldsymbol{r}_1$, and $\boldsymbol{r}_2$) of the fourth-order moment is defined by

$$\hat{\mu}(z, \boldsymbol{\xi}_1, \boldsymbol{\xi}_2, \boldsymbol{\zeta}_1, \boldsymbol{\zeta}_2; \tau) = \iint_{\mathbb{R}^2\times\mathbb{R}^2\times\mathbb{R}^2\times\mathbb{R}^2} \mu(z, \boldsymbol{q}_1, \boldsymbol{q}_2, \boldsymbol{r}_1, \boldsymbol{r}_2; \tau) \times \exp(-i\boldsymbol{q}_1 \cdot \boldsymbol{\xi}_1 - i\boldsymbol{q}_2 \cdot \boldsymbol{\xi}_2 - i\boldsymbol{r}_1 \cdot \boldsymbol{\zeta}_1 - i\boldsymbol{r}_2 \cdot \boldsymbol{\zeta}_2)\mathrm{d}\boldsymbol{q}_1\mathrm{d}\boldsymbol{q}_2\mathrm{d}\boldsymbol{r}_1\mathrm{d}\boldsymbol{r}_2. \tag{A6}$$

It satisfies

$$\begin{aligned}\frac{\partial \hat{\mu}}{\partial z} + \frac{i}{k_o}(\boldsymbol{\xi}_1 \cdot \boldsymbol{\zeta}_1 + \boldsymbol{\xi}_2 \cdot \boldsymbol{\zeta}_2)\hat{\mu} &= \frac{\sigma_m^2 k_o^2 \ell_m^3}{4(2\pi)^2}\int_{\mathbb{R}^2} \hat{C}(\boldsymbol{k}\ell_m)[\hat{\mu}(\boldsymbol{\xi}_1 - \boldsymbol{k}, \boldsymbol{\xi}_2 - \boldsymbol{k}, \boldsymbol{\zeta}_1, \boldsymbol{\zeta}_2) \\ &+ \hat{\mu}(\boldsymbol{\xi}_1 + \boldsymbol{k}, \boldsymbol{\xi}_2 - \boldsymbol{k}, \boldsymbol{\zeta}_1, \boldsymbol{\zeta}_2) - 2\hat{\mu}(\boldsymbol{\xi}_1, \boldsymbol{\xi}_2, \boldsymbol{\zeta}_1, \boldsymbol{\zeta}_2) \\ &+ g_\tau\hat{\mu}(\boldsymbol{\xi}_1 + \boldsymbol{k}, \boldsymbol{\xi}_2, \boldsymbol{\zeta}_1, \boldsymbol{\zeta}_2 - \boldsymbol{k}) + g_\tau\hat{\mu}(\boldsymbol{\xi}_1 - \boldsymbol{k}, \boldsymbol{\xi}_2, \boldsymbol{\zeta}_1, \boldsymbol{\zeta}_2 - \boldsymbol{k}) \\ &- g_\tau\hat{\mu}(\boldsymbol{\xi}_1, \boldsymbol{\xi}_2 - \boldsymbol{k}, \boldsymbol{\zeta}_1, \boldsymbol{\zeta}_2 - \boldsymbol{k}) - g_\tau\hat{\mu}(\boldsymbol{\xi}_1, \boldsymbol{\xi}_2 + \boldsymbol{k}, \boldsymbol{\zeta}_1, \boldsymbol{\zeta}_2 - \boldsymbol{k})]\mathrm{d}\boldsymbol{k},\end{aligned} \tag{A7}$$

starting from

$$\begin{aligned}\hat{\mu}(z=0, \boldsymbol{\xi}_1, \boldsymbol{\xi}_2, \boldsymbol{\zeta}_1, \boldsymbol{\zeta}_2; \tau) &= (2\pi)^8 \phi_{\ell_s^{-1}}(\boldsymbol{\xi}_1)\phi_{\ell_s^{-1}}(\boldsymbol{\xi}_2)\delta(\boldsymbol{\zeta}_1)\delta(\boldsymbol{\zeta}_2) \\ &+ (2\pi)^8 f_\tau^2 \phi_{\ell_s^{-1}}(\boldsymbol{\xi}_1)\phi_{\ell_s^{-1}}(\boldsymbol{\zeta}_2)\delta(\boldsymbol{\zeta}_1)\delta(\boldsymbol{\xi}_2).\end{aligned} \tag{A8}$$

Here $\hat{C}(\boldsymbol{q}) = \int_{\mathbb{R}^2} C(\boldsymbol{\chi}) \exp(i\boldsymbol{q} \cdot \boldsymbol{\chi})\mathrm{d}\boldsymbol{\chi}$ is the Fourier transform of C,

$$\phi_\kappa(\boldsymbol{\xi}) = \frac{1}{2\pi\kappa^2} \exp\left(-\frac{|\boldsymbol{\xi}|^2}{2\kappa^2}\right) \tag{A9}$$

is the two-dimensional centered isotropic Gaussian density with standard deviation κ, δ is the Dirac delta distribution, and f_τ, g_τ are defined in Eq. (20). We now seek to characterize

$$\mu_4(L, \mathbf{0}, \mathbf{0}, \mathbf{0}, \mathbf{0}; \tau) = \mu(L, \mathbf{0}, \mathbf{0}, \mathbf{0}, \mathbf{0}; \tau) = \frac{1}{(2\pi)^8} \iint_{\mathbb{R}^2\times\mathbb{R}^2\times\mathbb{R}^2\times\mathbb{R}^2} \times \hat{\mu}(L, \boldsymbol{\xi}_1, \boldsymbol{\xi}_2, \boldsymbol{\zeta}_1, \boldsymbol{\zeta}_2; \tau)\mathrm{d}\boldsymbol{\xi}_1\mathrm{d}\boldsymbol{\xi}_2\mathrm{d}\boldsymbol{\zeta}_1\mathrm{d}\boldsymbol{\zeta}_2. \tag{A10}$$

Due to the special initial condition that is proportional to $\delta(\boldsymbol{\zeta}_1)$, the solution $\hat{\mu}$ to Eq. (A7) is itself proportional to $\delta(\boldsymbol{\zeta}_1)$, and we can therefore reduce the problem Eq. (A7) to the analysis of

$$\hat{\eta}(z, \boldsymbol{\xi}_2, \boldsymbol{\zeta}_2; \tau) = \frac{1}{(2\pi)^4} \iint_{\mathbb{R}^2\times\mathbb{R}^2} \hat{\mu}(z, \boldsymbol{\xi}_1, \boldsymbol{\xi}_2, \boldsymbol{\zeta}_1, \boldsymbol{\zeta}_2; \tau) \mathrm{d}\boldsymbol{\xi}_1 \mathrm{d}\boldsymbol{\zeta}_1. \tag{A11}$$

The quantity of interest is then

$$\mu_4(L, \mathbf{0}, \mathbf{0}, \mathbf{0}, \mathbf{0}; \tau) = \frac{1}{(2\pi)^4} \iint_{\mathbb{R}^2\times\mathbb{R}^2} \hat{\eta}(L, \boldsymbol{\xi}_2, \boldsymbol{\zeta}_2; \tau) \mathrm{d}\boldsymbol{\xi}_2 \mathrm{d}\boldsymbol{\zeta}_2. \tag{A12}$$

The function $\hat{\eta}(z, \boldsymbol{\xi}_2, \boldsymbol{\zeta}_2)$ is a solution to the characteristic system

$$\begin{aligned} \frac{\partial \hat{\eta}}{\partial z} + \frac{i}{k_o} \boldsymbol{\xi}_2 \cdot \boldsymbol{\zeta}_2 \hat{\eta} = \frac{\sigma_m^2 k_o^2 \ell_m^3}{4(2\pi)^2} \int_{\mathbb{R}^2} & \hat{C}(\boldsymbol{k}\ell_m)[-2\hat{\eta}(\boldsymbol{\xi}_2, \boldsymbol{\zeta}_2) \\ & + 2\hat{\eta}(\boldsymbol{\xi}_2 - \boldsymbol{k}, \boldsymbol{\zeta}_2) + 2g_\tau \hat{\eta}(\boldsymbol{\xi}_2, \boldsymbol{\zeta}_2 \\ & - \boldsymbol{k}) - g_\tau \hat{\eta}(\boldsymbol{\xi}_2 - \boldsymbol{k}, \boldsymbol{\zeta}_2 - \boldsymbol{k}) \\ & - g_\tau \hat{\eta}(\boldsymbol{\xi}_2 + \boldsymbol{k}, \boldsymbol{\zeta}_2 - \boldsymbol{k})]\mathrm{d}\boldsymbol{k}, \end{aligned} \tag{A13}$$

starting from

$$\hat{\eta}(z=0, \boldsymbol{\xi}_2, \boldsymbol{\zeta}_2; \tau) = (2\pi)^4 \phi_{\ell_s^{-1}}(\boldsymbol{\xi}_2)\delta(\boldsymbol{\zeta}_2) + (2\pi)^4 f_\tau^2 \phi_{\ell_s^{-1}}(\boldsymbol{\zeta}_2)\delta(\boldsymbol{\xi}_2). \tag{A14}$$

This simplified system of Eqs. (A13) and (A14) underlies the scintillation results presented above. Note that the fourth-moment problem has been reduced to a problem defined relative to two, rather than four, copies of the lateral spatial variables. We derive explicit solutions to this system in different scaling regimes in Appendix B.

APPENDIX B: DERIVATION OF SCINTILLATION RESULTS

As mentioned in Section 2.B, the Itô–Schrödinger equation is valid in the white-noise paraxial regime, when the wavelength is much smaller than the correlation radii of the source and of the medium, which are themselves much smaller than the propagation distance. By the Itô–Schrödinger equation, the fourth-order moment Eq. (21) satisfies a closed Eq. (22). In this appendix, we derive closed form expressions of the solution to Eq. (22) in three special white-noise paraxial regimes, depending on the ratio of the correlation radii of the source and of the medium.

B.1. Scintillation Regime with a Large Correlation Radius of the Source

We consider the white-noise paraxial regime in which, additionally, the correlation radius of the source is larger than the correlation radius of the medium $\ell_s \gg \ell_m$ and derive the results presented in Section 4.A. More exactly, we here deal with the following scaled regime:

$$\frac{\ell_m}{\ell_s} \sim \varepsilon, \quad \frac{L}{\ell_s} \sim \alpha^{-1}, \quad \frac{\lambda_o}{\ell_s} \sim \alpha\varepsilon, \quad \sigma_m^2 \sim \alpha^3 \varepsilon, \tag{B1}$$

and we assume $\alpha \ll \varepsilon \ll 1$ (note that $L/\ell_{\mathrm{sc}} \sim 1$ and $\lambda_o L/\ell_m^2 \sim \varepsilon^{-1}$). This means that the paraxial white-noise limit $\alpha \to 0$ is taken first (and we get an ε-dependent Itô–Schrödinger equation), and then we want to apply the limit $\varepsilon \to 0$ in the fourth-moment Eq. (A13). In view of Eq. (B1), it is natural to introduce the rescaled function

$$\tilde{\eta}^\varepsilon(z, \boldsymbol{\xi}_2, \boldsymbol{\zeta}_2; \tau) = \hat{\eta}\left(\frac{z}{\varepsilon}, \boldsymbol{\xi}_2, \boldsymbol{\zeta}_2; \tau\right) \exp\left(i\frac{z}{\varepsilon k_o}\boldsymbol{\xi}_2 \cdot \boldsymbol{\zeta}_2\right). \tag{B2}$$

In the regime Eq. (B1), the rescaled function $\tilde{\eta}^\varepsilon$ satisfies the equation with fast phases:

$$\frac{\partial \tilde{\eta}^\varepsilon}{\partial z} = \mathcal{L}_z^\varepsilon \tilde{\eta}^\varepsilon, \tag{B3}$$

where

$$\begin{aligned} \mathcal{L}_z^\varepsilon \tilde{\eta}(\boldsymbol{\xi}_2, \boldsymbol{\zeta}_2) = \frac{\sigma_m^2 k_o^2 \ell_\mathrm{m}^3}{4(2\pi)^2} \int_{\mathbb{R}^2} & \hat{C}(\boldsymbol{k}\ell_m) \\ & \Big[-2\tilde{\eta}(\boldsymbol{\xi}_2, \boldsymbol{\zeta}_2) + 2\tilde{\eta}(\boldsymbol{\xi}_2 - \boldsymbol{k}, \boldsymbol{\zeta}_2) e^{i\frac{z}{\varepsilon k_o}\boldsymbol{k}\cdot\boldsymbol{\zeta}_2} \\ & + 2g_\tau \tilde{\eta}(\boldsymbol{\xi}_2, \boldsymbol{\zeta}_2 - \boldsymbol{k}) e^{i\frac{z}{\varepsilon k_o}\boldsymbol{k}\cdot\boldsymbol{\xi}_2} \\ & - g_\tau \tilde{\eta}(\boldsymbol{\xi}_2 - \boldsymbol{k}, \boldsymbol{\zeta}_2 - \boldsymbol{k}) e^{i\frac{z}{\varepsilon k_o}(\boldsymbol{k}\cdot(\boldsymbol{\zeta}_2 + \boldsymbol{\xi}_2) - |\boldsymbol{k}|^2)} \\ & - g_\tau \tilde{\eta}(\boldsymbol{\xi}_2 - \boldsymbol{k}, \boldsymbol{\zeta}_2 + \boldsymbol{k}) e^{i\frac{z}{\varepsilon k_o}(\boldsymbol{k}\cdot(\boldsymbol{\zeta}_2 - \boldsymbol{\xi}_2) + |\boldsymbol{k}|^2)}\Big] \mathrm{d}\boldsymbol{k}, \end{aligned} \tag{B4}$$

and the initial condition is

$$\begin{aligned} \tilde{\eta}^\varepsilon(z=0, \boldsymbol{\xi}_2, \boldsymbol{\zeta}_2; \tau) = {} & (2\pi)^4 \phi_{\varepsilon/\ell_s}(\boldsymbol{\xi}_2)\delta(\boldsymbol{\zeta}_2) \\ & + (2\pi)^4 f_\tau^2 \phi_{\varepsilon/\ell_s}(\boldsymbol{\zeta}_2)\delta(\boldsymbol{\xi}_2). \end{aligned} \tag{B5}$$

Note that ϕ_κ belongs to L^1 and has an L^1-norm equal to one. The asymptotic behavior as $\varepsilon \to 0$ of the moments is therefore determined by the solutions to partial differential equations with rapid phase terms. We can now proceed as in [10], and we obtain the following proposition.

Proposition B.1. In the regime Eq. (B1), the function $\tilde{\eta}^\varepsilon(z, \boldsymbol{\xi}_2, \boldsymbol{\zeta}_2; \tau)$ has the form

$$\begin{aligned} \tilde{\eta}^\varepsilon(z, \boldsymbol{\xi}_2, \boldsymbol{\zeta}_2; \tau) = {} & K(z)\phi_{\varepsilon/\ell_s}(\boldsymbol{\xi}_2)\delta(\boldsymbol{\zeta}_2) + K(z)A_1(z, \boldsymbol{\xi}_2, \mathbf{0})\delta(\boldsymbol{\zeta}_2) \\ & + K(z)A_{g_\tau}\left(z, \boldsymbol{\zeta}_2, \frac{\boldsymbol{\xi}_2}{\varepsilon}\right)\phi_{\varepsilon/\ell_s}(\boldsymbol{\xi}_2) \\ & + f_\tau^2 K(z)\delta(\boldsymbol{\xi}_2)\phi_{\varepsilon/\ell_s}(\boldsymbol{\zeta}_2) \\ & + f_\tau^2 K(z)A_{g_\tau}(z, \boldsymbol{\zeta}_2, \mathbf{0})\delta(\boldsymbol{\xi}_2) \\ & + f_\tau^2 K(z)A_1\left(z, \boldsymbol{\xi}_2, \frac{\boldsymbol{\zeta}_2}{\varepsilon}\right)\phi_{\varepsilon/\ell_s}(\boldsymbol{\zeta}_2) \\ & + R^\varepsilon(z, \boldsymbol{\xi}_2, \boldsymbol{\zeta}_2; \tau), \end{aligned} \tag{B6}$$

where the functions K and A_g are defined by

$$K(z) = (2\pi)^4 \exp\left(-\frac{\sigma_\mathrm{m}^2 k_o^2 \ell_\mathrm{m} z}{2}\right), \tag{B7}$$

$$A_g(z,\boldsymbol{\xi},\boldsymbol{\zeta}) = \frac{1}{(2\pi)^2}\int_{\mathbb{R}^2} \times \left[\exp\left(\frac{\sigma_m^2 k_o^2 \ell_m g}{2}\int_0^z C\left(\frac{\boldsymbol{x}}{\ell_m}+\frac{\boldsymbol{\zeta} z'}{k_o \ell_m}\right)\mathrm{d}z'\right)-1\right] \times \exp(-i\boldsymbol{\xi}\cdot\boldsymbol{x})\mathrm{d}\boldsymbol{x}, \tag{B8}$$

and the function R^ε *satisfies* $\sup_{z\in[0,L]}\| R^\varepsilon(z,\cdot,\cdot;\tau)\|_{L^1(\mathbb{R}^2\times\mathbb{R}^2)} \overset{\varepsilon\to 0}{\to} 0$.

We remark that

$$\frac{K^{1/4}(z)}{2\pi} = \exp\left(-\frac{\sigma_m^2 k_o^2 \ell_m z}{8}\right) \tag{B9}$$

represents the effective damping of the mean wave field and transfer of coherent energy to incoherent wave energy in the case of a frozen medium and deterministic sources. We remark moreover that the factor A_g depends on the two-point statistics of the random medium at lateral offsets and captures effects of lateral scattering of wave field energy. As a result, the quantity of interest in Eq. (A12) is then

$$\mu_4^\varepsilon(L,\mathbf{0},\mathbf{0},\mathbf{0},\mathbf{0};\tau) = 1 + f_\tau^2\exp\left(-\frac{\sigma_m^2(1-g_\tau)k_o^2\ell_m L}{2}\right) + \mathcal{Q}_{g_\tau}(L) + f_\tau^2\mathcal{Q}_1(L), \tag{B10}$$

with

$$\mathcal{Q}_g(L) = \exp\left(-\frac{\sigma_m^2 k_o^2 \ell_m L}{2}\right)\int_{\mathbb{R}^2}\phi_{\ell_s^{-1}}(\boldsymbol{\zeta}) \times \left[\exp\left(\frac{\sigma_m^2 k_o^2 \ell_m g}{2}\int_0^L C\left(\frac{\boldsymbol{\zeta} z}{k_o\ell_m}\right)\mathrm{d}z\right)-1\right]\mathrm{d}\boldsymbol{\zeta}. \tag{B11}$$

Therefore, the relative covariance of the intensities at time zero and time τ is

$$\frac{\mu_4^\varepsilon(L,\mathbf{0},\mathbf{0},\mathbf{0},\mathbf{0};\tau)-\mu_2^\varepsilon(L,\mathbf{0},\mathbf{0};0)^2}{\mu_2^\varepsilon(L,\mathbf{0},\mathbf{0};0)^2} = f_\tau^2\exp\left(-\frac{\sigma_m^2(1-g_\tau)k_o^2\ell_m L}{2}\right) + \mathcal{Q}_{g_\tau}(L) + f_\tau^2\mathcal{Q}_1(L). \tag{B12}$$

This gives the result Eq. (26) for the scintillation index in the regime $\ell_s \gg \ell_m$.

B.2. Scintillation Regime with an Intermediate Correlation Radius of the Source

We consider the white-noise paraxial regime in which, additionally, the correlation radius of the source is of the same order as the correlation radius of the medium $\ell_s \sim \ell_m$. This is the regime when the source lateral spatial fluctuations take place on the same scale of variation as that of random microstructure fluctuations, rather than being large relative to this scale as in Section B.1. More exactly, we here deal with the following scaled regime:

$$\frac{\ell_m}{\ell_s}\sim 1,\quad \frac{L}{\ell_s}\sim\alpha^{-1}\varepsilon^{-1},\quad \frac{\lambda_o}{\ell_s}\sim\alpha,\quad \sigma_m^2\sim\alpha^3\varepsilon, \tag{B13}$$

and we assume $\alpha \ll \varepsilon \ll 1$ (note that $L/\ell_{\mathrm{sc}}\sim 1$ and $\lambda_o L/\ell_m^2 \sim \varepsilon^{-1}$). This means that the paraxial white-noise limit $\alpha\to 0$ is taken first, and then we want to apply the limit $\varepsilon\to 0$ in the fourth-moment Eq. (A13). As above, we introduce the rescaled function

$$\tilde{\eta}^\varepsilon(z,\boldsymbol{\xi}_2,\boldsymbol{\zeta}_2;\tau) = \hat{\eta}\left(\frac{z}{\varepsilon},\boldsymbol{\xi}_2,\boldsymbol{\zeta}_2;\tau\right)\exp\left(i\frac{z}{k_o\varepsilon}\boldsymbol{\xi}_2\cdot\boldsymbol{\zeta}_2\right). \tag{B14}$$

In the regime Eq. (B13), the rescaled function $\tilde{\eta}^\varepsilon$ satisfies again the equations with fast phases, Eqs. (B3) and (B4), here with the initial condition given by Eq. (A14). The asymptotic behavior as $\varepsilon\to 0$ of the moments is therefore determined by the solutions to partial differential equations with rapid phase terms. We can again proceed similarly as in [10], and we obtain the following proposition.

Proposition B.2. In the scintillation regime Eq. (B13), the function $\tilde{\eta}^\varepsilon(z,\boldsymbol{\xi}_2,\boldsymbol{\zeta}_2;\tau)$ *has the form*

$$\tilde{\eta}^\varepsilon(z,\boldsymbol{\xi}_2,\boldsymbol{\zeta}_2;\tau) = (2\pi)^4 B_1(z,\boldsymbol{\xi}_2)\delta(\boldsymbol{\zeta}_2) + (2\pi)^4 f_\tau^2 B_{g_\tau}(z,\boldsymbol{\zeta}_2)\delta(\boldsymbol{\xi}_2) + R^\varepsilon(z,\boldsymbol{\xi}_2,\boldsymbol{\zeta}_2;\tau), \tag{B15}$$

with

$$B_g(z,\boldsymbol{\xi}) = \frac{1}{(2\pi)^2}\int_{\mathbb{R}^2} \exp\left(-i\boldsymbol{\xi}\cdot\boldsymbol{x} - \frac{|\boldsymbol{x}|^2}{2\ell_s^2} - \frac{\sigma_m^2 k_o^2\ell_m z}{2}\left[1-gC\left(\frac{\boldsymbol{x}}{\ell_m}\right)\right]\right)\mathrm{d}\boldsymbol{x}, \tag{B16}$$

and the function R^ε *satisfies* $\sup_{z\in[0,L]}\| R^\varepsilon(z,\cdot,\cdot;\tau)\|_{L^1(\mathbb{R}^2\times\mathbb{R}^2)} \overset{\varepsilon\to 0}{\to} 0$.

As a result, the quantities of interest Eq. (A12) are

$$\mu_4^\varepsilon(L,\mathbf{0},\mathbf{0},\mathbf{0},\mathbf{0};\tau) = 1 + f_\tau^2\exp\left(-\frac{\sigma_{\mathrm{m}}^2(1-g_\tau)k_o^2\ell_{\mathrm{m}} L}{2}\right) \tag{B17}$$

and

$$\frac{\mu_4^\varepsilon(L,\mathbf{0},\mathbf{0},\mathbf{0},\mathbf{0};\tau)-\mu_2^\varepsilon(L,\mathbf{0},\mathbf{0};0)^2}{\mu_2^\varepsilon(L,\mathbf{0},\mathbf{0};0)^2} = f_\tau^2\exp\left(-\frac{\sigma_{\mathrm{m}}^2(1-g_\tau)k_o^2\ell_{\mathrm{m}} L}{2}\right). \tag{B18}$$

This then gives the result Eq. (35) for the scintillation index.

B.3. Scintillation Regime with a Small Correlation Radius of the Source

We finally consider the white-noise paraxial regime in which, additionally, the correlation radius of the source is smaller than the correlation radius of the medium $\ell_s \ll \ell_m$ and derive the result Eq. (37) for the scintillation index in this regime. More exactly, we here deal with the following scaled regime:

$$\frac{\ell_m}{\ell_s} \sim \varepsilon^{-1}, \quad \frac{L}{\ell_s} \sim \alpha^{-1}, \quad \frac{\lambda_o}{\ell_s} \sim \alpha, \quad \sigma_m^2 \sim \alpha^3 \varepsilon^{-1}, \quad \textbf{(B19)}$$

and we assume $\alpha \ll \varepsilon \ll 1$ (note that $L/\ell_{sc} \sim \varepsilon^{-2}$ and $\lambda_o L/\ell_s^2 \sim 1$). This means that the paraxial white-noise limit $\alpha \to 0$ is taken first, and then we want to apply the limit $\varepsilon \to 0$ in the fourth-moment Eq. (A13). We also assume that C is smooth and isotropic, so that we have Eq. (32), and also $\frac{1}{(2\pi)^2}\int_{\mathbb{R}^2} \hat{C}(\boldsymbol{q})\boldsymbol{q}\otimes\boldsymbol{q}d\boldsymbol{q} = 2c_2\mathbf{I}$. We denote by $\hat{\eta}^\varepsilon$ the function Eq. (A11) in the regime Eq. (B19). Then we find that in the regime of small ε, the function $\hat{\eta}^\varepsilon(z, \boldsymbol{\xi}_2, \boldsymbol{\zeta}_2; \tau)$ is a solution to the system

$$\frac{\partial \hat{\eta}^\varepsilon}{\partial z} + \frac{i}{k_o}\boldsymbol{\xi}_2 \cdot \boldsymbol{\zeta}_2 \hat{\eta}^\varepsilon = \frac{\sigma_m^2 k_o^2 c_2(1-g_\tau)}{2\ell_m}\Delta_{\xi_2}\hat{\eta}^\varepsilon, \quad \textbf{(B20)}$$

with the initial condition given by Eq. (A14). We can easily solve Eq. (B20) via a Fourier transform and find Proposition B.3.

Proposition B.3 In the scintillation regime Eq. (B19), *the function* $\hat{\eta}^\varepsilon(z, \boldsymbol{\xi}_2, \boldsymbol{\zeta}_2; \tau)$ *has the form*

$$\begin{aligned}\hat{\eta}^\varepsilon(z, \boldsymbol{\xi}_2, \boldsymbol{\zeta}_2; \tau) &= (2\pi)^4 G_1(z, \boldsymbol{\xi}_2; \tau)\delta(\boldsymbol{\zeta}_2) \\ &\quad + (2\pi)^4 f_\tau^2 G_2(z, \boldsymbol{\xi}_2, \boldsymbol{\zeta}_2; \tau)\phi_{1/\ell_s}(\boldsymbol{\zeta}_2),\end{aligned} \quad \textbf{(B21)}$$

with

$$\begin{aligned}G_1(z, \boldsymbol{\xi}_2; \tau) &= \frac{\ell_s^2}{2\pi}\frac{1}{1+\frac{\sigma_m^2(1-g_\tau)c_2k_o^2\ell_s^2 L}{\ell_m}} \\ &\quad \times \exp\left(-\frac{\ell_s^2|\boldsymbol{\xi}_2|^2}{2\left(1+\frac{\sigma_m^2(1-g_\tau)c_2k_o^2\ell_s^2 L}{\ell_m}\right)}\right),\end{aligned} \quad \textbf{(B22)}$$

$$\begin{aligned}G_2(z, \boldsymbol{\xi}_2, \boldsymbol{\zeta}_2; \tau) &= \frac{1}{(2\pi)^2}\int_{\mathbb{R}^2}\exp\left(-\frac{c_2(1-g_\tau)\sigma_m^2k_o^2}{2\ell_m}\int_0^L\left|\boldsymbol{x}-\frac{\boldsymbol{\zeta}_2 z}{k_o}\right|^2 \mathrm{d}z - i\boldsymbol{\xi}_2\cdot\boldsymbol{x}\right)\mathrm{d}\boldsymbol{x} \\ &= \frac{\ell_m}{2\pi c_2(1-g_\tau)\sigma_m^2k_o^2L}\exp\left(-\frac{iL}{2k_o}\boldsymbol{\xi}_2\cdot\boldsymbol{\zeta}_2\right)\exp\left(-\frac{c_2(1-g_\tau)\sigma_m^2L^3}{24\ell_m}|\boldsymbol{\zeta}_2|^2 - \frac{\ell_m}{2c_2(1-g_\tau)\sigma_m^2k_o^2L}|\boldsymbol{\xi}_2|^2\right).\end{aligned} \quad \textbf{(B23)}$$

As a result,

$$\mu_4^\varepsilon(L, \mathbf{0}, \mathbf{0}, \mathbf{0}, \mathbf{0}; \tau) = 1 + \frac{f_\tau^2}{1+\frac{c_2(1-g_\tau)\sigma_m^2L^3}{3\ell_m\ell_s^2}} \quad \textbf{(B24)}$$

and

$$\frac{\mu_4^\varepsilon(L, \mathbf{0}, \mathbf{0}, \mathbf{0}, \mathbf{0}; \tau) - \mu_2^\varepsilon(L, \mathbf{0}, \mathbf{0}; 0)^2}{\mu_2^\varepsilon(L, \mathbf{0}, \mathbf{0}; 0)^2} = \frac{f_\tau^2}{1+\frac{c_2(1-g_\tau)\sigma_m^2L^3}{3\ell_m\ell_s^2}}. \quad \textbf{(B25)}$$

This then gives Eq. (37) for the scintillation index when $\ell_s \ll \ell_m$.

Funding. Agence Nationale de la Recherche (ANR-19-CE46- 413 0007); National Science Foundation (DMS-2010046); Air Force Office of Scientific Research (FA9550-18-1-0217).

Acknowledgment. We thank C. Nelson, S. Avramov-Zamurovic, O. Korotkova, S. Guth, and R. Malek-Madani for allowing us to use their data from [12] to generate Fig. 7. J.G. was supported by the ANR and AFOSR. K.S. was supported by the AFOSR and the NSF.

Disclosures. The authors declare no conflicts of interest.

Data availability. Data underlying the results presented in Fig. 7 were published in [12]. No other data were analyzed in the presented research, and no data were generated.

REFERENCES

1. L. C. Andrews and R. L. Philipps, *Laser Beam Propagation through Random Media* (SPIE, 2005).
2. J. C. Dainty, *Laser Speckle and Related Phenomena*, Topics in Applied Physics (Springer-Verlag, 1975), Vol. **9**.
3. V. I. Tatarskii, A. Ishimaru, and V. U. Zavorotny, eds., *Wave Propagation in Random Media (Scintillation)* (SPIE, 1993).
4. H. Gercekcioglu and Y. Baykal, “Minimization of the scintillation index of sinusoidal Gaussian beams in weak turbulence for aerial vehicle-satellite laser communications,” J. Opt. Soc. Am. A **38**, 862–868 (2021).
5. G. Xu, Z. Song, and Q. Zhang, “Outage probability and channel capacity of an optical spherical wave propagating through anisotropic weak-to-strong oceanic turbulence with Málaga distribution,” J. Opt. Soc. Am. A **37**, 1622–1629 (2020).
6. G. Gbur, “Partially coherent beam propagation in atmospheric turbulence,” J. Opt. Soc. Am. A **31**, 2038–2045 (2014).
7. F. Wang, X. Liu, and Y. Cai, “Propagation of partially coherent beam in turbulent atmosphere: a review,” Prog. Electromagnet. Res. **150**, 123–143 (2015).
8. M. Charnotskiii, “Propagation of polarized waves in inhomogeneous media,” J. Opt. Soc. Am. A **33**, 1385–1394 (2016).
9. J. Garnier and K. Sølna, “Scintillation in the white-noise paraxial regime,” Commun. Partial Differential Equations **39**, 626–650 (2014).
10. J. Garnier and K. Sølna, “Fourth-moment analysis for beam propagation in the white-noise paraxial regime,” Arch. Rational Mech. Anal. **220**, 37–81 (2016).
11. S. Avramov-Zamurovic, C. Nelson, S. Guth, and O. Korotkova, “Flatness parameter influence on scintillation reduction for multi-Gaussian Schell-model beams propagating in turbulent air,” Appl. Opt. **55**, 3442–3446 (2016).
12. C. Nelson, S. Avramov-Zamurovic, O. Korotkova, S. Guth, and R. Malek-Madani, “Scintillation reduction in pseudo multi-Gaussian Schell model beams in the maritime environment,” Opt. Commun. **364**, 145–149 (2016).
13. X. Xiao and D. Voltz, “Wave optics simulation approach for partially spatially coherent beams,” Opt. Express **14**, 6986–6992 (2006).
14. G. Baker, “Gaussian beam weak scintillation: low-order turbulence effects and applicability of the Rytov method,” J. Opt. Soc. Am. A **23**, 395–417 (2006).
15. X. Shan, C. Menyuk, J. Chen, and Y. Ai, “Scintillation index analysis of an optical wave propagating through the moderate-to-strong turbulence in satellite communication links,” Opt. Commun. **445**, 255–261 (2019).

16. R. L. Fante, “Effect of source bandwidth and receiver response time on the scintillation index in random media,” Radio Sci. **12**, 223–229 (1977).
17. R. L. Fante, “The effect of source temporal coherence on light scintillations in weak turbulence,” J. Opt. Soc. Am. **69**, 71–73 (1979).
18. R. L. Fante, “Intensity fluctuations of an optical wave in a turbulent medium effect of source coherence,” Opt. Acta **28**, 1203–1207 (1981).
19. V. A. Banach, V. M. Buldakov, and V. L. Mironov, “Intensity fluctuations of the partially coherent light-beam in a turbulent atmosphere,” Opt. Spectrosc. **54**, 1054–1059 (1983).
20. V. A. Banakh and V. M. Buldakov, “Effect of the initial degree of light-beam spatial coherence on intensity fluctuations in turbulent atmospheres,” Opt. Spectrosc. **55**, 707–712 (1983).
21. Y. Baykal and M. A. Plonus, “Intensity fluctuations due to a spatially partially coherent source in atmospheric turbulence as predicted by Rytov’s method,” J. Opt. Soc. Am. A **2**, 2124–2132 (1985).
22. O. Korotkova, L. C. Andrews, and R. L. Phillips, “Model for a partially coherent Gaussian beam in atmospheric turbulence with application in Lasercom,” Opt. Eng. **43**, 330–341 (2004).
23. G. Bal and O. Pinaud, “Dynamics of wave scintillation in random media,” Commun. Partial Differential Equations **35**, 1176–1235 (2010).
24. S. E. J. Shaw, “Scintillation averaging and fade statistics,” J. Opt. Soc. Am. A **37**, 833–840 (2020).
25. M. Charnotskii, “Extended Huygens-Fresnel principle and optical waves propagation in turbulence: discussion,” J. Opt. Soc. Am. A **32**, 1357–1365 (2015).
26. M. Charnotskii, “Beam scintillations for ground-to-space propagation. Part I: Path integrals and analytic techniques,” J. Opt. Soc. Am. A **27**, 2169–2179 (2010).
27. G. C. Valley and D. L. Knepp, “Application of joint Gaussian statistics to interplanetary scintillation,” J. Geophys. Res. **81**, 4723–4730 (1976).
28. I. G. Yakushkin, “Moments of field propagating in randomly inhomogeneous medium in the limit of saturated fluctuations,” Radiophys. Quantum Electron. **21**, 835–840 (1978).
29. G. Bal, T. Komorowski, and L. Ryzhik, “Asymptotics of the solutions of the random Schrödinger equation,” Arch. Rational Mech. Anal. **200**, 613–664 (2011).
30. J.-P. Fouque, J. Garnier, G. Papanicolaou, and K. Sølna, *Wave Propagation and Time Reversal in Randomly Layered Media* (Springer, 2007).
31. Y. Gu and T. Komorowski, “Gaussian fluctuations from random Schrödinger equation,” Commun. Partial Differential Equations **46**, 201–232 (2021).
32. J. Garnier and K. Sølna, “Focusing waves through a randomly scattering medium in the white-noise paraxial regime,” SIAM J. Appl. Math. **77**, 500–519 (2017).
33. D. Voelz and K. Fitzhenry, “Pseudo-partially coherent beam for free-space laser communication,” Proc. SPIE **5550**, 218–224 (2004).
34. J. Garnier and K. Sølna, “Beaming through turbulence,” in *Imaging and Applied Optics 2019 (COSI, IS, MATH, pcAOP)*, OSA Technical Digest (2019), paper PTh2D.4.
35. J. Garnier and K. Sølna, “Coupled paraxial wave equations in random media in the white-noise regime,” Ann. Appl. Probab. **19**, 318–346 (2009).
36. A. Ishimaru, *Wave Propagation and Scattering in Random Media* (IEEE, 1997).
37. V. I. Tatarskii, “Light propagation in a medium with random refractive index inhomogeneities in the Markov random process approximation,” Sov. Phys. JETP **29**, 1133–1138 (1969).
38. S. M. Rytov, Y. A. Kravtsov, and V. I. Tatarskii, *Principles of Statistical Radiophysics 4. Wave Propagation through Random Media* (Springer, 1989).
39. J. Garnier and K. Sølna, “Scaling limits for wave pulse transmission and reflection operators,” Wave Motion **46**, 122–143 (2009).
40. J. Garnier and K. Sølna, “Imaging through a scattering medium by speckle intensity correlations,” Inverse Prob. **34**, 094003 (2018).
41. J.-P. Fouque, G. Papanicolaou, and Y. Samuelides, “Forward and Markov approximation: the strong-intensity-fluctuations regime revisited,” Waves Random Media **8**, 303–314 (1998).
42. B. J. Ucsinski, “Analytical solution of the fourth-moment equation and interpretation as a set of phase screens,” J. Opt. Soc. Am. A **2**, 2077–2091 (1985).
43. K. Furutsu, “Statistical theory of wave propagation in a random medium and the irradiance distribution function,” J. Opt. Soc. Am. **62**, 240–251 (1972).
44. V. I. Tatarskii, “The effects of turbulent atmosphere on wave propagation,” TT-68-50464 (U.S. Department of Commerce, 1971).
45. D. Dawson and G. Papanicolaou, “A random wave process,” Appl. Math. Optim. **12**, 97–114 (1984).
46. L. Isserlis, “On a formula for the product-moment coefficient of any order of a normal frequency distribution in any number of variables,” Biometrika **12**, 134–139 (1918).
47. M. I. Charnotskii, “Common omissions and misconceptions of wave propagation in turbulence: discussion,” J. Opt. Soc. Am. A **29**, 711–721 (2012).
48. K. Furutsu and Y. Furuhama, “Spot dancing and relative saturation phenomena of irradiance scintillation of optical beams in a random medium,” Optica **20**, 707–719 (1973).